

See discussions, stats, and author profiles for this publication at: <https://www.researchgate.net/publication/234009359>

Moderating Strain without Sacrificing Reactivity: Design of Fast and Tunable Noncatalyzed Alkyne–Azide Cycloadditions via Stereoelectronically Controlled Transition State Stabiliza...

ARTICLE in JOURNAL OF THE AMERICAN CHEMICAL SOCIETY · DECEMBER 2012

Impact Factor: 12.11 · DOI: 10.1021/ja3114196 · Source: PubMed

CITATIONS

35

READS

36

3 AUTHORS:



Brian Gold

University of Wisconsin–Madison

14 PUBLICATIONS 185 CITATIONS

SEE PROFILE



Gregory Dudley

Florida State University

102 PUBLICATIONS 1,508 CITATIONS

SEE PROFILE



Igor Alabugin

Florida State University

142 PUBLICATIONS 3,583 CITATIONS

SEE PROFILE

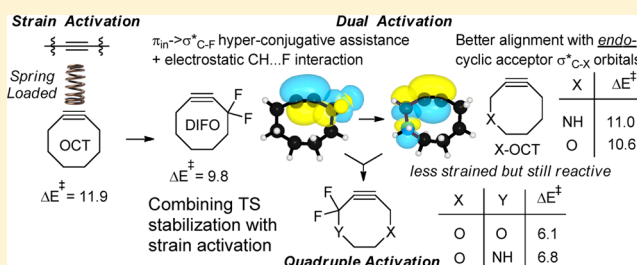
Moderating Strain without Sacrificing Reactivity: Design of Fast and Tunable Noncatalyzed Alkyne–Azide Cycloadditions via Stereoelectronically Controlled Transition State Stabilization

Brian Gold, Gregory B. Dudley, and Igor V. Alabugin*

Department of Chemistry and Biochemistry, Florida State University, Tallahassee, Florida, 32306-4390, United States

S Supporting Information

ABSTRACT: Recently, we have identified two strategies for selective transition state (TS) stabilization in catalyst-free azide/alkyne cycloadditions. In particular, the transition states for the formation of both 1,4- and 1,5-isomers can be stabilized via hyperconjugative assistance for the C \cdots N bond formation, whereas the 1,5-TS can be stabilized via C–H \cdots X H-bonding interactions. When the hyperconjugative assistance is maximized by the antiperiplanar arrangement of propargylic σ -acceptors relative to the forming bonds, the combination of these TS-stabilizing effects was predicted to lead to ~ 1 million fold acceleration of the cycloaddition with methyl azide. The present work investigated whether hyperconjugative assistance and H-bonding can be combined with strain activation for the design of even more reactive alkynes and whether reactivity can be turned “on demand.” When stereoelectronic amplification is achieved by optimal positioning of σ -acceptors at the endocyclic bonds antiperiplanar to the breaking alkyne π -bonds, the stabilization of the bent alkyne geometry leads to a significant decrease in strain in cyclic alkynes *without* compromising their reactivity in alkyne–azide cycloadditions. The approach can be used in a modular fashion where the TS stabilizing effects are introduced sequentially until the desired level of reactivity is achieved. A significant increase in reactivity upon the protonation of an endocyclic NH-group suggests a new strategy for the design of click reactions triggered by a pH-change or introduction of an external Lewis acid.



INTRODUCTION

The applications of “click chemistry”¹ range from drug design² and chemical biology³ to materials science,⁴ development of sensors,⁵ polymer chemistry⁶ and other molecular sciences. Although the copper-catalyzed variant^{7,8} of the Huisgen azide–alkyne cycloaddition (CuAAC)⁹ is arguably the most widely utilized “click reaction,”¹⁰ the toxicity of copper salts limits the utility of this fast and versatile process for *in vivo* applications.¹¹ In addition, the negative impact of copper salts on the luminescent properties of nanocrystals presents a problem in the application of click chemistry to the functionalization of quantum dots and related nanomaterials.^{12,13}

Bertozzi,¹⁴ Boons,^{3b,15} and others¹⁶ have harnessed the reactivity of activated cyclooctynes (OCT) in strain-promoted¹⁷ azide–alkyne cycloadditions (SPAAC) as metal-free alternatives to the CuAAC with reactivity suitable for a variety of applications (Figure 1).^{18,19} For example, Bertozzi and co-workers demonstrated that intracellular azide–cyclooctyne coupling occurs within hours at room temperature^{3a,20} and enables *in vivo* biological imaging.²¹ Boons introduced dibenzocyclooctyne (DIBO) reagents,¹² where further reactivity enhancements over cyclooctyne are achieved due to an increase in ring strain (more sp^2 -centers) and, in collaboration with Popik,¹⁵ developed a way to generate DIBO photochemically. Rutjes, Van Delft and co-workers introduced additional strain via cyclopropane fusion.^{16a} In an effort to “brush against the line between stability and

reactivity without crossing it,” Bertozzi reported that lactam-based BARAC provides a 10-fold increase in reactivity over DIBO, leading to intracellular coupling within minutes.²²

Although the above examples clearly illustrate the potential of reactant destabilization in the design of reactive alkynes,²³ they also illustrate the drawback inherent to this approach: the relatively low stability of the most reactive compounds, some of which “should be stored as a solid at 0 °C protected from light and oxygen.”²² In contrast, transition state stabilization, the alternative strategy favored by many of Nature’s powerful catalysts,²⁴ provides reaction acceleration without sacrificing the stability of reactants.

Initial indications that such stabilization is possible were given by the important observation by Bertozzi et al. that the reactivity of OCT is enhanced >50-fold by incorporation of fluorine atoms at the propargylic position (cf. DIFO, Figure 1).²⁵ The ~ 2 kcal/mol decrease in the activation barrier for DIFO relative to cyclooctyne is reproduced by DFT computations.²⁶ Recently, we have shown that the accelerating effects of propargylic fluorine substituents are manifested via different mechanisms: hyperconjugative assistance for 1,4-addition and Me \cdots F interaction for 1,5-addition (Figure 2).²⁷

Received: November 20, 2012

Published: December 31, 2012

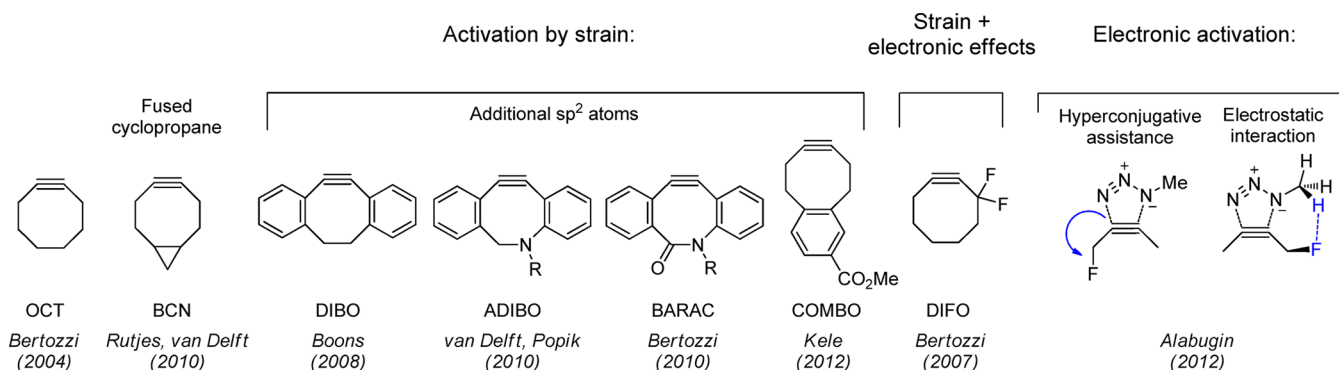


Figure 1. Literature approaches to alkynes with increased reactivity in noncatalyzed cycloaddition with azides.

Electronic effects accelerating DIFO / azide cycloadditions:

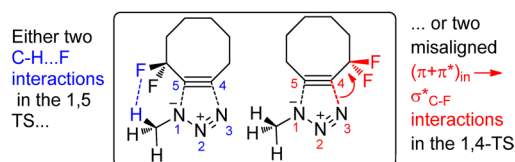


Figure 2. Competing electronic effects responsible for the rate acceleration of DIFO/azide cycloadditions relative to those with OCT.

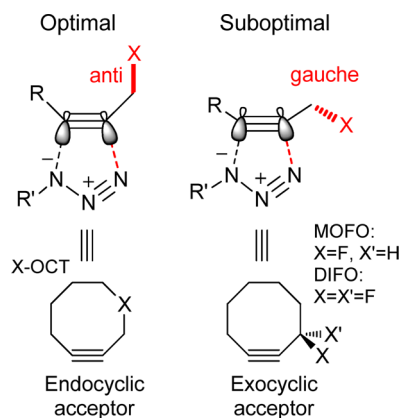


Figure 3. Optimal (antiperiplanar) and suboptimal (gauche) arrangements between propargylic σ -acceptors X and the reacting alkyne π -bond (top). Stereoelectronic differences between the endocyclic and exocyclic acceptors (bottom).

DIFO cannot fully benefit from the combination of the two TS-stabilizing effects identified in our previous work because cyclic restraints render the optimal antiperiplanar position of a C–F bond impossible (*vide infra*). Each of the two regioisomeric transition states for the methyl azide/DIFO cycloaddition relies mostly on one effect at a time: (a) either C–H...F interactions in the 1,5-TS or (b) imperfect hyperconjugative assistance from the two gauche C–F bonds in the 1,4-TS.

Intriguingly, TS stabilization provided by a *single antiperiplanar* propargylic fluorine substituent in the acyclic substrate (1-fluorobut-2-yne) is *greater* than the TS stabilization provided by *two gauche* fluorines in DIFO. This difference stems from the hyperconjugative origin of TS stabilization which is fully displayed when the proper overlap between orbitals is achieved (Figure 3).²⁸

The greater impact of the antiperiplanar arrangement of the σ^*_{C-F} acceptor and the in-plane alkyne π -system illustrates the stereoelectronic nature of the hyperconjugative assistance. It lowers the TS energy via two effects: (a) decrease in the energy

cost for alkyne bending (distortion energy) needed to reach the cycloaddition TS geometry and (b) assistance to the bond formation. Not only does the alkyne π -orbital donor ability increase upon bending,²⁷ but also the interaction of the alkyne LUMO and azide HOMO leads to orbital mixing which partially redirects the electron density to the alkyne π^* . An appropriately positioned propargylic σ^* or π^* acceptor assists in delocalizing this electron density, facilitating the C...N bond formation and providing selective cycloaddition TS stabilization²⁷ (Figure 4). This interaction is not perfect for DIFO, but is fully manifested when the σ acceptor is antiperiplanar (*app*).

The hyperconjugative assistance can be complemented by the stabilizing C–H...F contacts which can be considered H-bonds with a significant electrostatic component (Figure 5). These two independent mechanisms can be combined to achieve an even larger acceleration once additional σ -acceptors are introduced. Remarkably, the proper positioning of just three C–F bonds at the propargylic carbons eliminates $\sim 80\%$ of the barrier difference between 2-butyne and cyclooctyne without introducing strain destabilization in the reactant.

An intriguing conclusion from these results is that the “economic” utilization of the two electronic effects outlined above leaves free positions at the propargylic carbons which can be further functionalized for additional control, suggesting that even greater reaction acceleration may be possible (Figure 6). In this work, we will investigate whether activation of alkynes via *transition state stabilization* can be combined with *reactant destabilization* for the design of very reactive cycloalkynes with tunable reactivity (Figure 7).

In the first part, we will combine strain with the accelerating effects of *endocyclic* σ -acceptors in the cyclooctyne frame and determine if the two effects are compatible. If two conceptually different accelerating effects can be combined in such a way that selective transition state stabilization via stereoelectronic hyperconjugative effects and electrostatic CH...X interactions can complement reactant destabilization via strain and alkyne distortion, one can achieve the needed compromise between stability and reactivity in the design of alkyne reagents for click chemistry. In the second part, we will show that the combination of effects can indeed lead to extraordinarily low activation barriers for the click cycloadditions.

COMPUTATIONAL DETAILS

The computational analysis of potential energy profiles for azide–alkyne cycloadditions was performed at the B3LYP/6-31G(d) level of theory using Gaussian 03 software.²⁹ For 1,3-dipolar cycloadditions, B3LYP/6-31G(d) and B3LYP/6-31+G(d,p) have mean absolute deviation of 1.5 and 2.6 kcal/mol, respectively, relative to the highly accurate

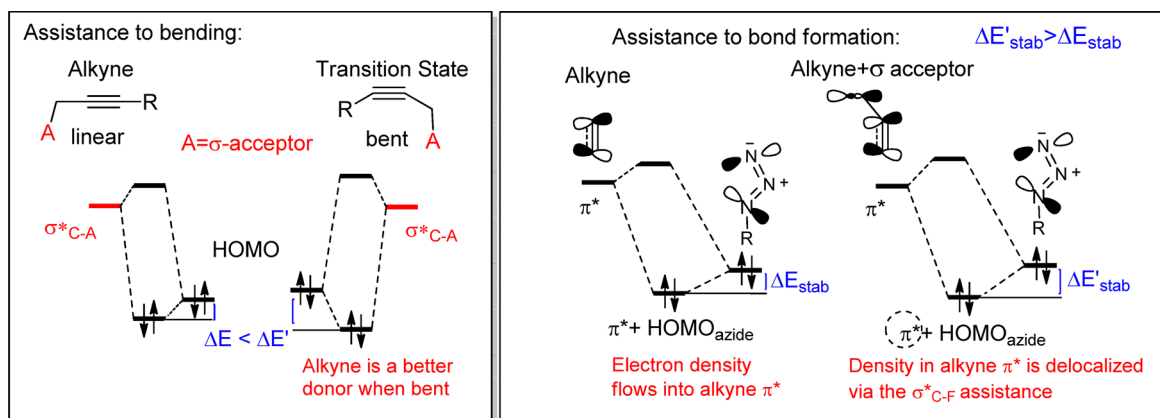


Figure 4. Two components to the stereoelectronic assistance to alkyne-azide cycloadditions: “assistance to bending” is a consequence of increased donor ability of distorted π -bonds, “assistance to bond formation” delocalizes electron density enhancing the C–N bond forming LUMO_{alkyne}/HOMO_{azide} interaction.

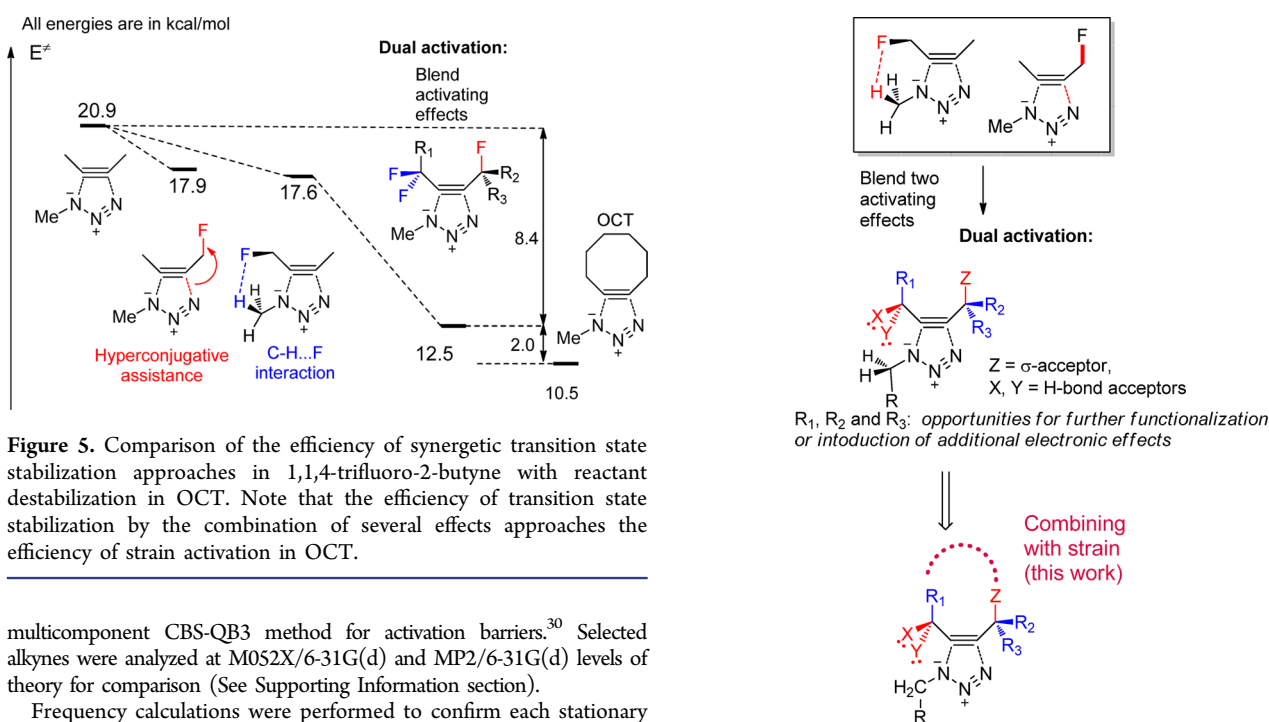


Figure 5. Comparison of the efficiency of synergistic transition state stabilization approaches in 1,1,4-trifluoro-2-butyne with reactant destabilization in OCT. Note that the efficiency of transition state stabilization by the combination of several effects approaches the efficiency of strain activation in OCT.

multicomponent CBS-QB3 method for activation barriers.³⁰ Selected alkynes were analyzed at M052X/6-31G(d) and MP2/6-31G(d) levels of theory for comparison (See Supporting Information section).

Frequency calculations were performed to confirm each stationary point as minima or first-order saddle points. Solvation corrections were performed on the gas phase geometries (unless otherwise noted) at the B3LYP/6-31G(d) level of theory. A CPCM dielectric continuum solvent model for acetonitrile and water with UA0 radii was used previously by Houk and co-workers for related cycloadditions.^{26b} This model does not explicitly include nonelectrostatic contributions, cavitation, and dispersion energies and should be considered as the first approximation of solvation effects.³¹

Electronic structures of reactants and transition states were analyzed using Natural Bond Orbital (NBO) analysis. The NBO 4.0³² program was used to evaluate the energies of hyperconjugative interactions. The NBO analysis transforms the canonical delocalized Hartree–Fock (HF) MOs, or corresponding natural orbitals of a correlated description into localized orbitals that are closely tied to chemical bonding concepts. Filled NBOs describe the hypothetical strictly localized Lewis structure. The interactions between filled and vacant orbitals represent the deviation of the molecule from the Lewis structure and can be used as a measure of delocalization.^{23,33} This method gives energies of hyperconjugative interactions both by deletion of the off-diagonal Fock matrix elements between the interacting orbitals and from the second order perturbation approach:

$$E(2) = -n_{\sigma} \frac{\langle \sigma / F \sigma^* \rangle^2}{\epsilon_{\sigma^*} - \epsilon_{\sigma}} = -n_{\sigma} \frac{F_{ij}^2}{\Delta E} \quad (1)$$

Figure 6. Favorable placement of fluorine substituents for optimal activation via cooperative effects and further possible variations in the design of reactive alkynes with suitable activation patterns.

where $\langle \sigma / F \sigma^* \rangle$, or F_{ij} is the Fock matrix element between the i and j NBO orbitals, ϵ_{σ} and ϵ_{σ^*} are the energies of σ and σ^* NBO's, and n_{σ} is the population of the donor σ orbital.^{34,35} From the NBO analysis, overlap integrals were obtained from the preorthogonalized NBOs. Detailed descriptions of the NBO calculations are available in the literature.^{36,37}

Chair and Boat Transition States. Analysis of different conformations in both the starting material and TS show that the chair conformation is preferred in both the starting cyclooctynes as well as in the TS. This is consistent with earlier reports of a preference for the chair conformation for DIFO at all levels of theory, while the boat TS may compete in OCT, since this geometry is favored at some levels of theory.^{26b} In all cases shown in Figure 8, the boat TS is higher in energy. On the basis of the Curtin–Hammett postulate,³⁸ one can anticipate that these reactions should proceed through the chair TS.

The lower activation barriers for the boat TSs is due to lower distortion energies of reactants needed to reach the transition states (distortion analysis is provided in the Supporting Information,

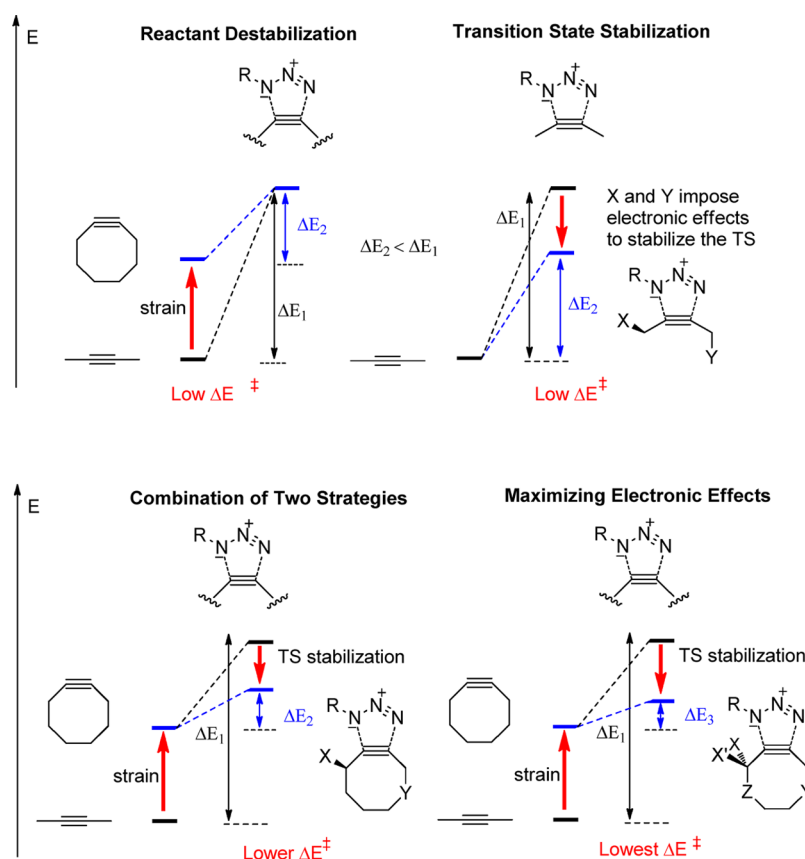


Figure 7. Comparison of alternative strategies for acceleration of copper-free click reactions.

Figure S2 and Table S4). It is possible that by constraining the starting alkynes in the boat conformation even more reactive alkynes could be designed through additional strain activation. Fox and co-workers found that a similar strategy can be effective in tetrazine/trans-cyclooctene cycloadditions.³⁹ We will investigate this possibility in our future work. In the present manuscript, however, all discussion will be centered on chair conformations.

RESULTS AND DISCUSSION

Endocyclic Substitution Alleviates Strain without Sacrificing Reactivity. Reactivity is only one of the challenges in the design of alkynes for click chemistry. Another important challenge is selectivity. Although cycloalkyne strain accelerates cycloadditions, many highly reactive cycloalkynes are relatively unstable and prone to unselective reactivity. In order to understand the effect of heteroatom introduction on the strain in cyclooctyne framework, we had evaluated strain energies in heterocyclooctynes following approach described earlier by Bach^{26d,40} (Table 1).

The ~2 kcal/mol lower strain of DIFO relative to that of cyclooctyne (20.6 and 18.6 kcal/mol, respectively) is counter-intuitive. One would expect DIFO to be more strained than OCT because the fluorinated propargylic carbon of DIFO uses two ~sp² hybrids for making the endocyclic C–C bonds. This hybridization effect (which is a consequence of the Bent's rule)⁴¹ is analogous to adding an sp² carbon in the cyclooctyne framework, something which is usually used to increase strain in cyclooctynes.

The origin for the decreased strain becomes obvious upon the inspection of strain energies in cyclooctynes with endocyclic heteroatoms at the propargylic positions (X-OCT, Table 1). Remarkably, all of the X-Oct alkynes have SEs that are even

lower than the SE of DIFO!⁴² In fact, some of endocyclic heteroatoms bring the SEs close to the 12.4 kcal/mol^{26d,43} SE of cyclooctane.

The low strain reflects the effect of endocyclic hyperconjugation on stabilization of alkyne bending. The lower penalty for the alkyne bending in DIFO is due to hyperconjugative $\pi \rightarrow \sigma^*_{C-F}$ interactions with the exocyclic acceptors.

The greater hyperconjugative effect of a single acceptor C–X bond in X-OCT relative to the effect of two C–F bonds of DIFO illustrates the stereoelectronic nature of this phenomenon, which favors the antiperiplanar donor/acceptor arrangement.

Although endocyclic heteroatoms decrease strain in the cyclooctyne framework, the molecules are still destabilized relatively to Z-cyclooctenes (SE 6.8 kcal/mol) and, as the result, strain should still impose an accelerating effect on the cycloadditions. However, since strain is moderated by the presence of endocyclic heteroatoms, such systems may be easier to prepare and handle. Moreover, the combination of TS stabilization with reactant destabilization by strain may allow one to prepare alkynes which are not only more reactive than DIFO but also may be tunable via conformational and electronic effects.

TS Stabilization in Cycloalkynes with Endocyclic Acceptors. Considering findings from the previous section, one has to wonder whether the decreased strain in X-OCT alkynes may be detrimental for their reactivity in cycloadditions with azides. In this section, we will investigate the effect of stereoelectronically optimized hyperconjugative assistance by endocyclic σ -acceptors. On the basis of our previous findings,²⁷ we anticipated substitution at both propargylic carbons to impose an accelerating effect, with the acceptor positioned at

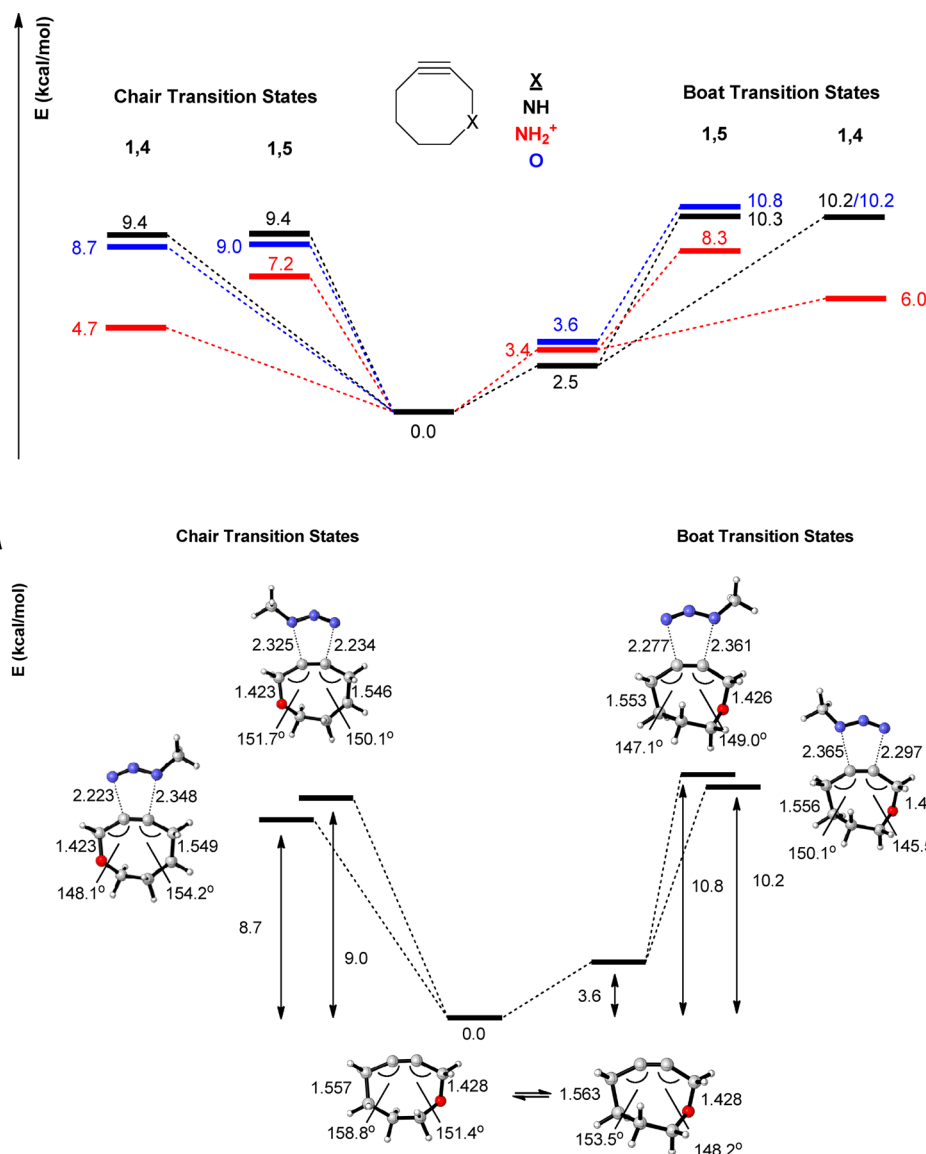


Figure 8. (Top) Relative energies of the chair and boat conformations of heterocycles featuring endocyclic propargylic σ -acceptors and their cycloadditions with methyl azide optimized at the B3LYP/6-31G(d) level of theory. (Bottom) Geometries of the chair and boat TSs for the “1,4” and “1,5” cycloaddition of O-OCT and methyl azide optimized at the B3LYP/6-31G(d) level of theory. Angles are given in degrees, bond distances in angstroms.

the propargylic carbon *opposite* to the azide alkyl group being more effective.

We began our analysis by comparing the effect of a single *endocyclic* acceptor⁴⁴ to the effect of two fluorine atoms in DIFO (Figure 9). The stereoelectronic nature of hyperconjugation suggests that the effect of σ -acceptors will be fully manifested only when they are aligned properly with the donor. As long as C–F bonds in DIFO are misaligned with the reacting alkyne π -system, they cannot impose their accelerating effect to the full capacity. In contrast, *endocyclic* σ -acceptors are antiperiplanar to the in-plane alkyne π -orbital. Although C–F bonds cannot be included into a cycle, we have shown previously that hyperconjugative acceptor ability of some σ -bonds (in particular C–N⁺) can rival the acceptor ability of C–F bonds.⁴⁵

Indeed, the computations predicted significant acceleration as the propargylic CH₂ group of cycloctyne is substituted by heteroatoms (Figure 9, Table 2). In the gas phase, this acceleration surpasses the effect of the *exocyclic* fluorines in DIFO.

Although the barriers become much closer after solvation is incorporated, the effect is still significant. Notably, in the 1,4-TS, a single properly aligned oxygen is as efficient as the two fluorines in DIFO. The extent of *endocyclic* activation is directly proportional to the acceptor ability of the activating group. This opens a number of intriguing approaches for fine-tuning click reactivity via electronic effects of substituents, metal coordination or protonation.⁴⁶ The latter possibility is illustrated by the effect of the endocyclic NH₂⁺ at the propargylic carbon (C–N⁺ is a strong σ -acceptor).^{35,47}

Distortion Analysis. To understand the origin of the accelerating effects deeper, we have utilized distortion analysis which has been used successfully by Houk and co-workers toward a variety of cycloadditions.^{26a,b,48} This analysis dissects the activation barrier for cycloadditions into distortion and interaction energies. Distortion describes the energy penalty for adopting the TS geometry by the reactants, whereas interaction energy reflects energy lowering due to covalent and noncovalent

Table 1. Strain Energies (SEs) of Cyclooctynes Discussed in This Work^a

R	X	Y	SE (kcal/mol)	SE (kcal/mol) H ₂ O ^{b,c}
OCT:				
H	CH ₂	CH ₂	20.4	20.6
DIFO:				
F	CH ₂	CH ₂	19.1	18.6
X - OCT				
H	O	CH ₂	16.3	16.7
H	NH	CH ₂	17.9	18.0
H	NH ₂ ⁺	CH ₂	18.2	16.4
X,Y - OCT				
H	O	O	12.9	13.8
H	NH	NH	18.5	18.3
H	NH ₂ ⁺	NH ₂ ⁺	46.0	20.9
H	O	NH	14.4	14.7
H	O	NH ₂ ⁺	19.0	15.2
Hybrids:				
F	O	CH ₂	15.3	15.5
F	NH	CH ₂	16.4	15.9
F	NH ₂ ⁺	CH ₂	19.9	16.7
F	O	O	14.1	14.1
F	NH	NH	17.4	16.8
F	NH ₂ ⁺	NH ₂ ⁺	46.8	21.0
F	O	NH	16.1	15.8
F	NH	O	16.6	15.6
F	O	NH ₂ ⁺	16.8	13.4
F	NH ₂ ⁺	O	24.0	17.6

^aNote that SE of cyclooctane and Z-cyclooctene is 12.4 and 6.8 kcal/mol, respectively.^{26d} ^bGas phase geometry. ^cCPCM (dielectric continuum solvent model), Radii = UA0.

interaction between the reactants. These results are summarized in Table 2.

As expected for all cyclic alkynes, the distortion energies are small indicating that the reactant geometries are already close to the bent geometry of the cycloaddition TS. The distortion energies for O-OCT and NH-OCT are slightly lower than those in OCT and DIFO, whereas the distortion energy for the NH₂⁺-OCT TS is slightly higher because this molecular structure is influenced stronger by the large interaction energy. Single point solvation correction decreases the interaction energy but it still remains substantial.

Because endocyclic substituents modify both the distortion and the interaction energies, a clear dissection of these effects is difficult, especially considering that azide distortion energies vary as well (from 13.7 to 15.4 kcal/mol in the gas phase). However, the combined distortion energies for all azide/X-OCT transition states are lower than they are for the cyclooctyne TS.

Similar to our earlier findings,²⁷ the increase of TS stabilization through an increase in interaction energies (*E*_{int} in Table 2) leads to deviations in the usually reliable^{26b} correlation of distortion energies with full activation barriers (Figure 10). The particularly large deviations observed for 1,5 DIFO TS (due to C–H...F interactions described in the introduction) and both 1,4 and 1,5-TS for NH₂⁺-OCT indicate the particularly strong intermolecular interactions between the two reacting species.

Because stabilization energies are greater than alkyne distortions, the NH₂⁺-OCT alkyne has a low overall barrier despite having the greatest distortion energy (the 1,5-TS). Considering the likely diminishing effect of solvation on the stabilization energies, we have fully reoptimized this TS with solvation included. As expected, the distortion decreased significantly (red arrow in Figure 10) when the stabilizing effect of intermolecular electrostatic interactions is diminished because the reacting system has to find a new compromise between the

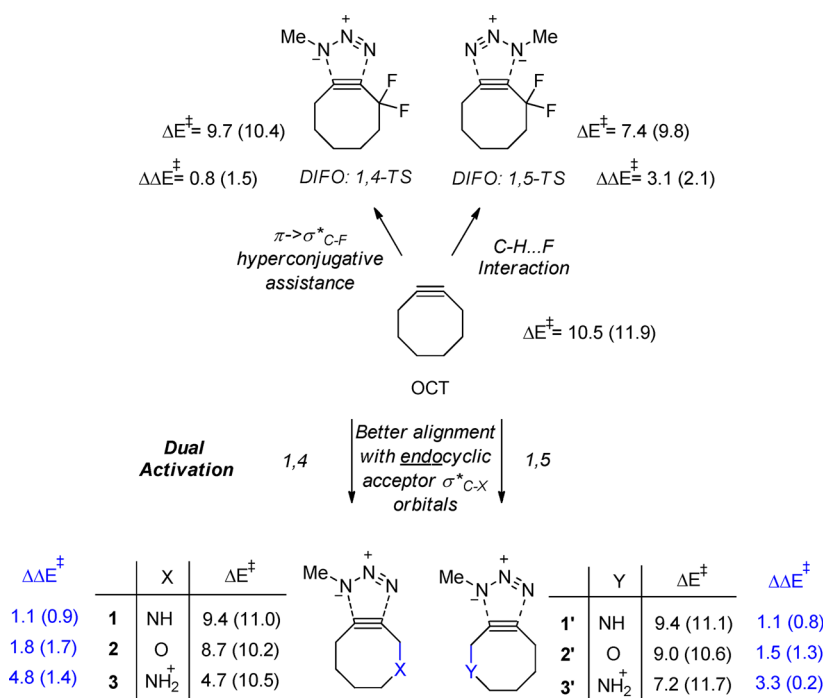
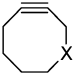


Figure 9. B3LYP/6-31G(d) activation energies of OCT, DIFO and heterocyclooctynes featuring endocyclic propargylic σ -acceptors. CPCM (water) solvation corrections are given in parentheses. $\Delta\Delta E^\ddagger$ values for X-OCT are shown relative to OCT to illustrate the effect of X on reactivity.

Table 2. Activation, Reaction, Distortion, And Interaction Energies for OCT, DIFO, and Heterocyclooctynes Featuring Endocyclic Propargylic σ -Acceptors: Geometries Optimized at the B3LYP/6-31G(d) Level of Theory

	ΔE^\ddagger , kcal/mol	ΔE_{RMS} , kcal/mol	E_{Dist} Alkyne, kcal/mol	E_{Dist} Azide, kcal/mol	E_{Dist} Total, kcal/mol	E_{int} , kcal/mol
X - OCT	Gas phase $\text{H}_2\text{O}^{a,b}$	Gas phase $\text{H}_2\text{O}^{a,b}$	Gas phase $\text{H}_2\text{O}^{a,b}$	Gas phase $\text{H}_2\text{O}^{a,b}$	Gas phase $\text{H}_2\text{O}^{a,b}$	Gas phase $\text{H}_2\text{O}^{a,b}$
Cyclooctyne	10.5	-79.0	2.1	15.3	17.4	-6.9
	11.9		1.9	15.5	17.5	-5.6
DIFO	7.4	-81.9	2.3	13.8	16.0	-8.7
1,5	9.8	-82.1	2.1	13.9	16.1	-6.3
DIFO	9.8	-78.5	2.3	14.1	16.5	-6.7
1,4	10.4	-82.1	2.2	14.4	16.6	-6.3
NH-OCT, 1	9.4	-80.4	1.6	14.3	16.0	-6.6
1,4	11.0	-82.9	1.6	14.6	16.2	-5.2
NH-OCT, 1'	9.4	-80.2	1.8	14.4	16.2	-6.7
1,5	11.1	-82.4	1.8	14.7	16.4	-5.3
O-OCT, 2	8.7	-83.4	1.5	13.7	15.2	-6.5
1,4	10.2	-85.2	1.5	13.9	15.4	-5.2
O-OCT, 2'	9.0	-82.7	1.9	13.9	15.7	-6.8
1,5	10.6	-84.8	1.9	14.1	16.0	-5.4
NH_2^+ -OCT, 3	4.7	-83.5	3.3	13.6	16.9	-12.2
1,4	10.5	-82.6	2.8	13.7	16.5	-6.1
NH_2^+ -OCT, 3'	7.2	-73.9	3.8	15.4	19.3	-12.0
1,5	11.7	-76.8	3.5	15.6	19.2	-7.5

^aGas phase geometry. ^bCPCM (dielectric continuum solvent model), Radii = UA0.

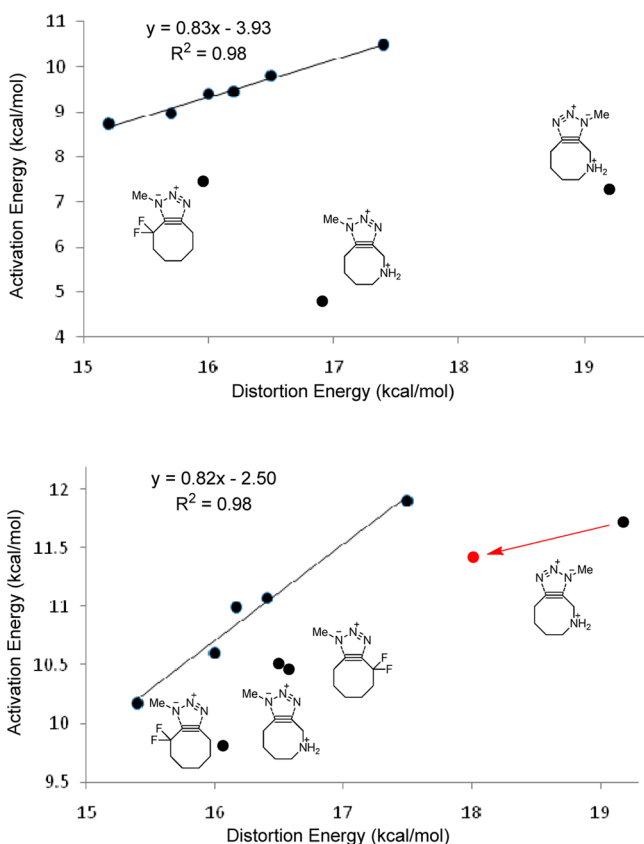


Figure 10. Correlation of the full distortion energy and activation energy cycloadditions between methyl azide with OCT, DIFO, and heterocyclooctynes featuring endocyclic propargylic σ -acceptors (Table 2, B3LYP/6-31G*). (Top) Gas phase data. (Bottom) Single point solvation (water) correction. Shown in red is the shift observed upon optimization in solution (data for all solvent optimizations is given in the Supporting Information Figure S1). The energies below the straight line deviate from the distortion plot due to selective TS stabilization (gas phase: $R^2 = 0.06$, if all nine points are included. CPCM (water): $R^2 = 0.56$, if all nine points are included).

conflicting energetic factors and requirements. Once the system could not benefit as much from the stabilization energy, it readjusted to decrease the distortion energy.

As in our previous work, placement of the propargylic acceptor at the C4 position provides greater stabilization in the TS. This selectivity parallels the acceptor strength, making NH_2^+ -OCT the most regioselective. Formation of the 1,4 regioisomer is more exothermic and has an earlier TS, requiring less energy to distort the azide to the TS geometry. This approach is also favored since the polarization of the alkyne is toward the acceptor moiety and N1 of the azide bears a greater negative charge than N3. In particular, full electrostatic analysis provided in the Supporting Information explains how the unfavorable combination of reactant dipoles renders the 1,5 NH_2^+ -OCT/TS and product less thermodynamically favorable.

NBO Dissection of Hyperconjugative Effects. The stereoelectronic advantage of endocyclic σ -acceptors is illustrated by the NBO plots for the three transition states involving DIFO and NH_2^+ -OCT (Figure 11). The NBO overlap integral, S_{ij} , quantifies the differences. In DIFO, the two $\sigma_{\text{C-F}}^*$ orbitals are positioned in a way where they interact with both in-plane and out-of plane alkyne π -bonds. However, the overlap with the out-of-plane π -system is more efficient (~ 0.2 au for each of the acceptors) than overlap with the in-plane π -system (~ 0.1 au). In the TS, one of the DIFO C-F bonds is reoriented to interact stronger with π_{in} in the DIFO TS, at the expense of weakening the interaction with the π_{out} alkyne orbital.⁴⁹ This, previously unrecognized, conformational effect leads to “switching on” of the $\pi_{\text{in}}/\pi_{\text{in}}^* \rightarrow \sigma_{\text{C-F}}^*$ hyperconjugative assistance in DIFO and illustrates the importance of this TS stabilizing effect. The relatively larger conformational change associated with this stereoelectronic adjustment is consistent with the slightly larger alkyne deformation energy for DIFO⁵⁰ in comparison to the 1,4-TS for the neutral X-OCT alkynes (Table 2) and with the more negative entropy of activation for DIFO in comparison to the other cycloalkynes (see the Supporting Information).

In contrast, overlap of the reacting alkyne π -bond with endocyclic acceptors is already “switched on” in the starting

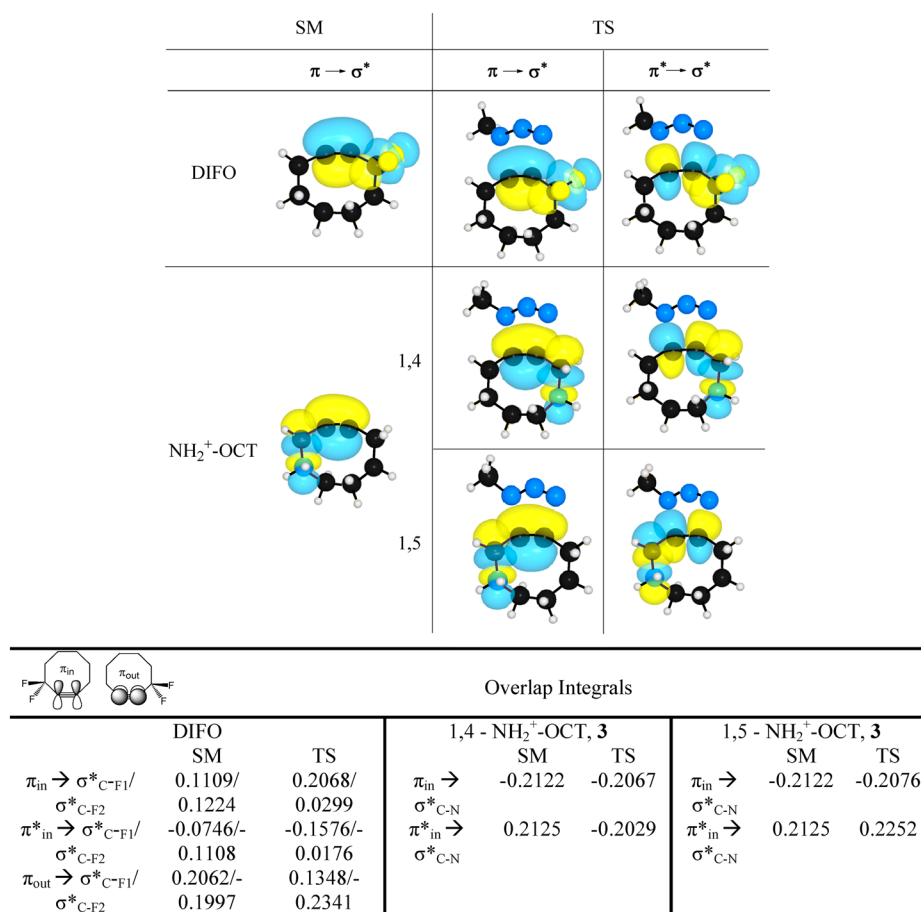


Figure 11. (Top) NBO plots for orbital interactions between the propargylic σ -acceptors and the reacting in-plane alkyne π -bond in the cycloaddition TSs of difluorocyclooctyne and NH₂⁺-OCT with methyl azide. (Bottom) Preorthogonal NBO overlap matrix elements between listed π orbitals and σ^*_{C-X} .

material (Figure 11). Although such stabilization of the reactants may be helpful for the preparation of these cyclic alkynes, this behavior appears to be less favorable than the conformational change in DIFO and would be unproductive unless this interaction gets stronger in the TS despite the overlap staying relatively constant. However, such increase is observed and endo substituents do impose a significant TS stabilizing effect (Table 3). We attribute this effect to two reasons: the lowering

Table 3. NBO Analysis (B3LYP/6-31G(d)) of Hyperconjugative Interactions Involved in the Methyl Azide Cycloaddition with Heterocyclooctynes Featuring Propargylic σ -Acceptors^a

$\pi + \pi^* \rightarrow \sigma^*$ energies, kcal/mol	starting alkyne	alkyne-TS geometry	full TS: alkyne + azide	hyperconjugative TS stabilization
OCT	2.9	3.0 (2.9) ^b	4.2 (3.7) ^b	1.2 (0.8)
DIFO	4.3	4.6 (4.6)	7.1 (6.6)	2.5 (2.0)
NH-OCT	5.1	5.3 (5.2)	5.6 (6.4)	0.3 (1.2)
O-OCT	7.2	7.5 (7.2)	8.8 (9.5)	1.3 (2.3)
NH ₂ ⁺ -OCT	9.2	9.9 (9.6)	17.0 (18.2)	7.1 (8.6)

^aOnly donation from the *in-plane* π -system (both π and π^*) is shown (kcal/mol). Values are for the 1,4-TS (1,5-TS). ^bValues given for each propargylic C-C bond.

of the energy gap between the interacting orbitals^{35,51} and an increase in the alkyne π^* population (as directly follows from

eq 1 given in the Computational Details section). This is readily illustrated by the relative NBO energies of stereoelectronic interactions in reactants and the TS (Table 3).⁵² While the $\pi_{in} \rightarrow \sigma^*_{C-F}$ overlap in DIFO is comparable to the $\pi_{in} \rightarrow \sigma^*_{C-N}$ in the NH₂⁺-OCT, the $\pi^*_{in} \rightarrow \sigma^*_{C-F}$ is much smaller than that of $\pi^*_{in} \rightarrow \sigma^*_{C-N}$ allowing for a greater assistance to bond formation in the latter case (Figure 4).

Let us analyze the reasons for this interesting behavior in more detail. We have reported earlier²⁷ that whereas a modest increase in the $\pi \rightarrow \sigma^*_{C-X}$ stabilization is observed upon bending of acyclic alkynes, a larger increase is found in the full TS where the azide moiety transfers electron density to the properly aligned acceptor via the alkyne π -system. The same is true for cyclic alkynes, except that the hyperconjugation increase associated with the additional reactant bending needed to reach the cycloaddition TS is even smaller. This is not surprising because the reactant geometry is much closer to the TS than it is for acyclic alkynes—very little additional bending is required.⁵³ The stereoelectronic nature is clearly evident when comparing the interactions of the misaligned acceptors in DIFO to those seen for the antiperiplanar arrangement in endo acceptors where the effects are maximized.

On the other hand, hyperconjugative stabilization is significantly increased in the full TS, where the azide is brought into close proximity of the bent alkyne moiety. In this case, the C-N bond forming interactions increase the population of the alkyne π_{in}^* orbital, the latter serving as a very efficient donor in

the interaction with the stereoelectronically aligned σ^* -acceptors (Figure 4, right panel). The increase in this interaction correlates well with the strength of the acceptor, ($\text{NH}_2^+ > \text{O} > \text{NH}$), revealing the potential for “on demand” activation through either protonation or metal coordination.

The NBO analysis also provides insights into the origin of regioselectivity for cycloadditions to X-OCT. Cycloaddition of the parent OCT molecule proceeds via a highly asynchronous TS where the incipient N3–C4 bond distance is considerably shorter than the N1–C5 distance (see Supporting Information for all geometries). In this TS, the propargylic C–C bond at the C4 end is slightly shorter (0.004 Å) than the analogous C5 bond. This observation is consistent with the slightly stronger interaction of the in plane π -system (π and π^*) with the anti-periplanar $\sigma^*_{\text{C5-C}}$ propargylic orbital than with the $\sigma^*_{\text{C4-C}}$ orbital (4.2 vs 3.7 kcal/mol). The analogous interactions in the full TS for the X-OCT alkynes 1–3 consistently suggest that hyperconjugation slightly favors the 1,5-TS and that the lower barriers for the 1,4-TS have to originate from a different factor. Comparison of electrostatic potentials for the alkyne and azide reactants (discussed in the previous section and summarized in the Supporting Information) indicates that 1,5-TS should be disfavored by the dipole–dipole interactions for the neutral alkynes where the heteroatom corresponds to the negative end of the dipole.

Triple Activation/Quadruple Activation. A potentially valuable feature of our approach is that activation can be accomplished in a modular fashion where each set of substituents leads to a progressive decrease in the activation barrier. Alkynes with dual activation are predicted to approach DIFO in reactivity. In this section, we will discuss alkynes with triple and quadruple activation patterns which are predicted to be even more reactive.

Triple activation can be provided in two different ways, illustrated in Figure 12 for $\text{X} = \text{O}$, either by introducing a second endocyclic acceptor or by combining hyperconjugative assistance by a single endocyclic acceptor with the $\text{C-H}\cdots\text{F}$ interactions. Finally, all four effects (strain, two endocyclic $\pi \rightarrow \sigma^*_{\text{C-X}}$ interactions and $\text{C-H}\cdots\text{F}$ contacts) can be combined in “superactivated alkynes.” These effects can be introduced in a modular way with a predictable outcome.

For example, the $\text{C-H}\cdots\text{F}$ interactions provide 3.1–3.7 kcal/mol barrier decrease (2.1–2.8 kcal/mol with solvation correction).⁵⁴ The 1,4-endocyclic C–O bonds contributes a little bit less: 1.8–2.4 (1.7–2.4 with solvation) kcal/mol. 1,5-hyperconjugative assistance is the smallest, but still a significant effect on the order of 0.9–1.6 (1.3–1.7 with solvation) kcal/mol.

Expansion of this modular approach to other endocyclic acceptors, X, increases the number of possibilities and provides cyclooctynes with a broad range of reactivities. The relative barrier lowering correlates with the acceptor properties of X: $\text{NH} < \text{O} < \text{NH}_2^+$. Our computational results for these systems are combined in Figure 13.

Because of the additional hyperconjugative assistance to both alkyne bending and bond formation, the activation barriers for systems with two endocyclic acceptors are further lowered both in the gas phase and in the solution. We see here a “super-activated” alkyne ($\text{X} = \text{Y} = \text{NH}_2^+$), appearing to have a negative barrier for the cycloadditions in the gas phase. This unusual result will be discussed below.

Interestingly, the two effects show cooperativity. In compounds 7–11, the exact magnitude of additional barrier lowering by the second acceptor Y depends also on the acceptor ability of

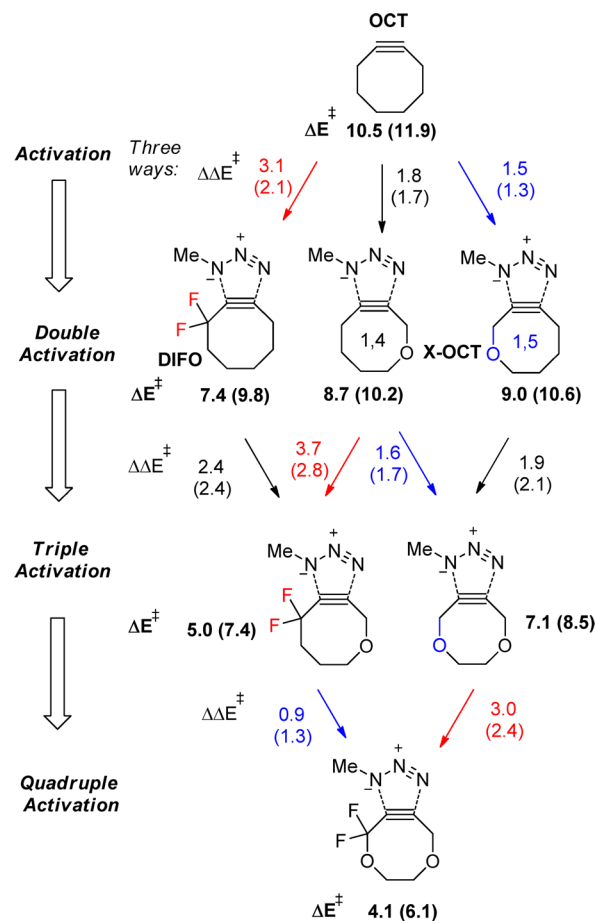


Figure 12. Modularity and cooperativity for the three transition state stabilization approaches for cycloadditions of substituted cyclooctynes and methyl azide. B3LYP/6-31G* activation energies (ΔE^\ddagger) are given in bold, changes in the activation barriers ($\Delta\Delta E^\ddagger$) introduced by an additional level of activation are given near the arrows. CPCM (water) solvation corrections are given in parentheses.

$\sigma^*_{\text{C-X}}$ as well. For instance, the magnitude of additional stabilization gained due to the incorporation of the $\sigma^*_{\text{C-O}}$ acceptor (alkynes 7, 8', and 9, $\text{Y} = \text{O}$) into compounds 1–3 increases with the acceptor ability of $\sigma^*_{\text{C-X}}$ (1.4 \rightarrow 1.7 \rightarrow 2.4 kcal/mol for $\text{NH} \rightarrow \text{O} \rightarrow \text{NH}_2^+$ in solution). Additionally, the incorporation of different $\sigma^*_{\text{C-X}}$ acceptors (alkynes 7, 8', and 9) into 2' ($\text{Y} = \text{O}$) provides greater additional stabilization (1.0 \rightarrow 2.1 \rightarrow 2.5 kcal/mol for $\text{NH} \rightarrow \text{O} \rightarrow \text{NH}_2^+$ in solution) than a single $\sigma^*_{\text{C-X}}$ acceptor (0.9 \rightarrow 1.7 \rightarrow 1.4 kcal/mol for $\text{NH} \rightarrow \text{O} \rightarrow \text{NH}_2^+$ in solution upon going from OCT to 1, 2, 3).

In addition, examination of the nonsymmetric alkynes (8, $\text{X} = \text{O}$, $\text{Y} = \text{NH}$ vs 8', $\text{X} = \text{NH}$, $\text{Y} = \text{O}$ and 9, $\text{X} = \text{NH}_2^+$, $\text{Y} = \text{O}$ vs 9', $\text{X} = \text{O}$, $\text{Y} = \text{NH}_2^+$) reveals the preference for the stronger acceptor to be anti to the azide's substituent, analogous to the preference of a single acceptor to be at the C4 carbon. This is also evident by the larger effect of protonation when the nitrogen is positioned properly (1.5 vs 0.6 kcal/mol in solution for the 8' \rightarrow 9 and 8 \rightarrow 9' pairs, respectively).

For the second mode of “triple activation” (“X-OCT+CF₂”), the magnitude of the additional barrier lowering due to fluorination of compounds 1, 2, and 3 also parallels the acceptor ability of X (2.5 \rightarrow 2.8 \rightarrow 4.1 kcal/mol for $\text{NH} \rightarrow \text{O} \rightarrow \text{NH}_2^+$ in 4–6), indicating positive synergy between the two effects.

Finally, the combination of strain, $\text{C-H}\cdots\text{F}$ interactions and both modes of hyperconjugative assistance (*quadruple activation*)

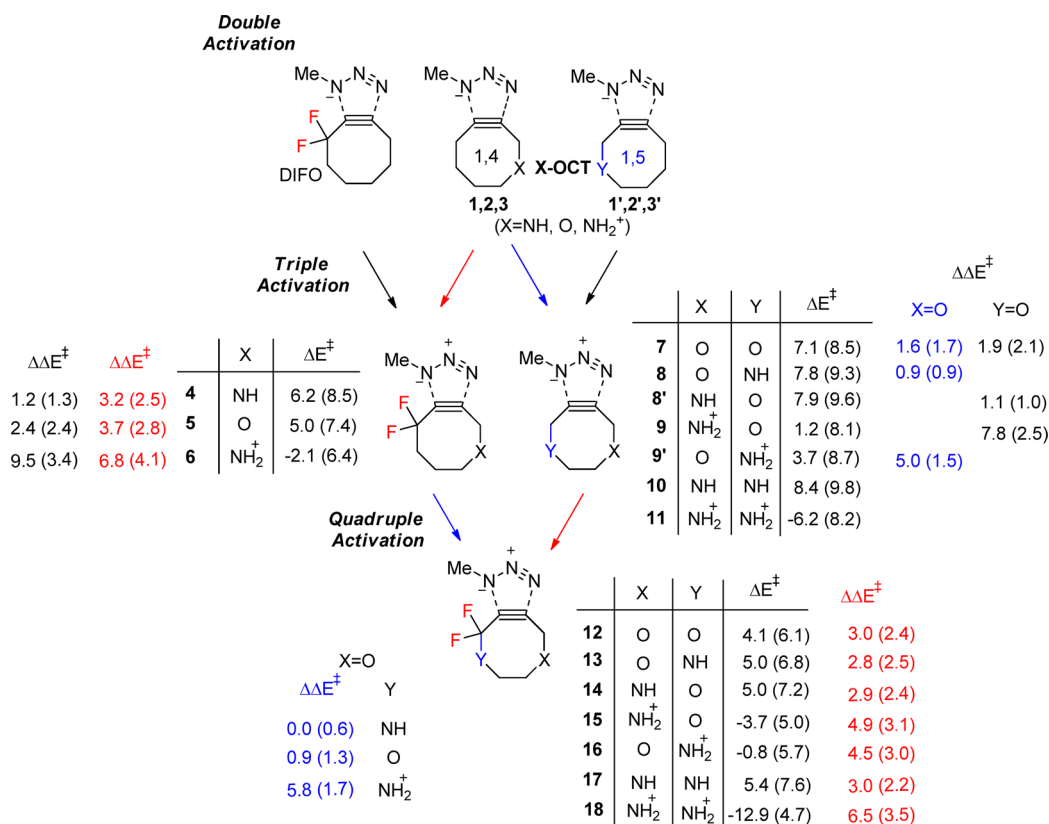


Figure 13. B3LYP/6-31G* activation energies of heterocyclooctynes combining multiple activating effects. CPCM (water) solvation corrections are given in parentheses. Color coding for stabilizing interactions: red, C–H...F; blue, 1,5-hyperconjugation; black, 1,4-hyperconjugation. For the sake of clarity, only the gas phase $\Delta\Delta E^\ddagger$ values are shown. Activation barriers for the additional regioisomers are given in the Supporting Information.

is the most efficient. Together, these effects result in unprecedented levels of reaction acceleration. The transition from alkynes 4, 5, and 6 to their analogues 12–18 gives similar barrier decrease for each of the σ^*_{C-Y} acceptors (0.8–0.9, 1.3–1.4, and 1.7 kcal/mol for Y = NH, O, and NH₂⁺, respectively). As seen upon going from *dual* to *triple* activation, the exact magnitude of additional decrease depends not only on the acceptor ability of Y (as expected: NH₂⁺ > O > NH) but also from the acceptor ability of σ^*_{C-X} as well.

The very large interaction energies for several “super-activated” cationic alkynes lead to the formation of an initial complex between reacting species prior to bond formation. As a result, the calculated energies of activation relative to the two isolated reactants in the gas phase are negative. When activation energies are recalculated relative to such complex or when solvation effects are included in the calculations, the activation barriers become positive. Since the overall goal of our structural design is to promote favorable interactions between the alkyne and the azide, formation of a complex lower in energy than the isolated reactants is not surprising.⁵⁵ As one would expect, the precomplexation is much stronger in the gas phase, but diminishes once solvation corrections are added, giving positive, albeit very low, activation barriers.

CONCLUSIONS

In summary, the combination of the two new strategies for selective TS stabilization in catalyst-free azide/alkyne cycloadditions with strain can be used to design highly reactive cycloalkynes for noncatalyzed alkyne–azide cycloadditions. Additional activation through external factors, such as protona-

tion and metal coordination, make these compounds attractive as candidates for “on demand” click chemistry. Importantly, fine-tuning of reactivity is possible through *dual*, *triple*, or *quadruple* activation which can be implemented in a modular fashion. Interestingly, even the “super-activated” alkynes are *less strained* than cyclooctyne and many reactive alkynes with acceptor heteroatoms at the endocyclic propargylic position are predicted to have strain energies close to cyclooctane. We are in a process of testing these predictions experimentally and plan to report our findings in the due course.

ASSOCIATED CONTENT

Supporting Information

Geometries, energies and distortion analysis for all reactants, products and transition states. This material is available free of charge via the Internet at <http://pubs.acs.org>.

AUTHOR INFORMATION

Corresponding Author

alabugin@chem.fsu.edu

Notes

The authors declare no competing financial interest.

ACKNOWLEDGMENTS

I.V.A. and G.B.D. are grateful to the National Science Foundation (Grants CHE-1152491 and CHE-0749918) for support of this research project.

REFERENCES

- (1) (a) Kolb, H. C.; Finn, M. G.; Sharpless, B. K. *Angew. Chem., Int. Ed.* **2001**, *40*, 2004. (b) Finn, M. G.; Fokin, V. V., Guest Eds. *Chem. Soc. Rev.* **2010**, *39*, 1221.
- (2) Tron, G. C.; Pirali, T.; Billington, R. A.; Canonico, P. L.; Sorba, G.; Genazzani, A. A. *Med. Res. Rev.* **2008**, *28*, 278.
- (3) (a) Jewett, J. C.; Bertozzi, C. R. *Chem. Soc. Rev.* **2010**, *39*, 1272. (b) Ning, X.; Guo, J.; Wolfert, M.; Boons, G.-J. *Angew. Chem., Int. Ed.* **2008**, *47*, 2253.
- (4) Binder, W. H.; Sachsenhofer, R. *Macromol. Rapid Commun.* **2007**, *28*, 15.
- (5) Huang, S.; Clark, R. J.; Zhu, L. *Org. Lett.* **2007**, *9*, 4999.
- (6) Golas, P. L.; Tsarevsky, N. V.; Sumerlin, B. S.; Matyjaszewski, K. *Macromolecules* **2006**, *39*, 6451.
- (7) Rostovtsev, V. V.; Green, L. G.; Fokin, V. V.; Sharpless, K. B. *Angew. Chem., Int. Ed.* **2002**, *41*, 2596.
- (8) Tornøe, C. W.; Christensen, C.; Meldal, M. *J. Org. Chem.* **2002**, *67*, 3057.
- (9) Huisgen, R. 1,3-Dipolar Cycloadditions—Introduction, Survey, Mechanism. In *1,3-Dipolar Cycloaddition Chemistry*; Padwa, A., Ed.; Wiley: New York, 1984; pp 1–176.
- (10) (a) Hein, J. E.; Fokin, V. V. *Chem. Soc. Rev.* **2010**, *39*, 1302. (b) Tornøe, C. W.; Meldal, M. *Chem. Rev.* **2008**, *108*, 2952. (c) Moses, J. E.; Moorhouse, A. D. *Chem. Soc. Rev.* **2007**, *36*, 1249.
- (11) The toxicity of Cu salts can be significantly alleviated by a suitable choice of Cu-coordinating ligands: Hong, V.; Steinmetz, N. F.; Manchester, M.; Finn, M. G. *Bioconjugate Chem.* **2010**, *21*, 1912.
- (12) Bernardin, A.; Cazet, A.; Guyon, L.; Delannoy, P.; Vinet, F.; Bonnaffe, D.; Texier, I. *Bioconjugate Chem.* **2010**, *21*, 583.
- (13) Han, H.-S.; Devaraj, N. K.; Lee, J.; Hilderbrand, S. A.; Weissleder, R.; Bawendi, M. G. *J. Am. Chem. Soc.* **2010**, *132*, 7838.
- (14) Codelli, J. A.; Baskin, J. M.; Agard, N. J.; Bertozzi, C. R. *J. Am. Chem. Soc.* **2008**, *130*, 11486.
- (15) (a) Poloukhine, A. A.; Mbua, N. E.; Wolfert, M. A.; Boons, G.-J.; Popik, V. V. *J. Am. Chem. Soc.* **2009**, *131*, 15769. (b) Sanders, B. C.; Friscourt, F.; Ledin, P. A.; Mbua, N. E.; Arumugam, S.; Guo, J.; Boltje, T. J.; Popik, V. V.; Boons, G.-J. *J. Am. Chem. Soc.* **2011**, *133*, 949.
- (16) (a) Dommerholt, J.; Schmidt, S.; Temming, R.; Hendricks, L. J. A.; Rutjes, F. P. J. T.; van Hest, J. C. M.; Lefebvre, D. J.; Friedl, P.; van Delft, F. L. *Angew. Chem. Int. Ed.* **2010**, *49*, 9422. (b) Becer, C. R.; Hoogenboom, R.; Schubert, U. S. *Angew. Chem., Int. Ed.* **2009**, *48*, 4900. (c) Varga, B. R.; Kállay, M.; Hegyi, K.; Béni, S.; Kele, P. *Chem.—Eur. J.* **2012**, *18*, 822. (d) Debets, M. F.; van Berkel, S. S.; Schoffelen, S.; Rutjes, F. P. J. T.; van Hest, J. C. M.; van Delft, F. L. *Chem. Commun.* **2010**, *46*, 97. (e) Kuzmin, A.; Poloukhine, A.; Wolfert, M. A.; Popik, V. V. *Bioconjugate Chem.* **2010**, *21*, 2076.
- (17) Wittig, G.; Krebs, A. *Chem. Ber.* **1961**, *94*, 3260.
- (18) Baskin, J. M.; Bertozzi, C. R. *Aldrichimica Acta* **2010**, *43*, 15.
- (19) Reviews on bioorthogonal chemistry: (a) Sletten, E. M.; Bertozzi, C. R. *Angew. Chem., Int. Ed.* **2009**, *48*, 6974. (b) Lim, R. K. V.; Lin, Q. *Chem. Commun.* **2010**, *46*, 1589. (c) Debets, M. F.; van Berkel, S. S.; Dommerholt, J.; Dirks, A. J.; Rutjes, F. P. J. T.; van Delft, F. L. *Acc. Chem. Res.* **2011**, *44*, 805. (d) Sletten, E. M.; Bertozzi, C. R. *Acc. Chem. Res.* **2011**, *44*, 666. (e) Best, M. D.; Rowland, M. M.; Bostic, H. E. *Acc. Chem. Res.* **2011**, *44*, 686.
- (20) Agard, N. J.; Prescher, J. A.; Bertozzi, C. R. *J. Am. Chem. Soc.* **2004**, *126*, 15046; *J. Am. Chem. Soc.* **2005**, *127*, 11196 (Addition/Correction).
- (21) Chang, P. V.; Prescher, J. A.; Sletten, E. M.; Baskin, J. M.; Miller, I. A.; Agard, N. J.; Lo, A.; Bertozzi, C. R. *Proc. Natl. Acad. Sci.* **2010**, *107*, 1821.
- (22) Jewett, J. C.; Sletten, E. M.; Bertozzi, C. R. *J. Am. Chem. Soc.* **2010**, *132*, 3688. See also: Jewett, J. C.; Bertozzi, C. R. *Org. Lett.* **2011**, *13*, 5937.
- (23) Reactant destabilization has been also used to activate alkynes in cycloaromatization reactions: (a) Nicolaou, K. C.; Zuccarello, G.; Ogawa, Y.; Schweiger, E. J.; Kumazawa, T. *J. Am. Chem. Soc.* **1988**, *110*, 4866. (b) Nicolaou, K. C.; Smith, A. L. *Acc. Chem. Res.* **1992**, *25*, 497. (c) Magnus, P.; Carter, P.; Elliott, J.; Lewis, R.; Harling, J.; Pittner, T.; Bauta, W. E.; Fortt, S. *J. Am. Chem. Soc.* **1992**, *114*, 2544. (d) Snyder, J. P. *J. Am. Chem. Soc.* **1990**, *112*, 5367. (e) Semmelhack, M. F.; Neu, T.; Foubelo, F. *J. Org. Chem.* **1994**, *59*, 5038. (f) Schreiner, P. R. *J. Am. Chem. Soc.* **1998**, *120*, 4184. (g) Schreiner, P. R. *Chem. Commun.* **1998**, 483. (h) Mita, T.; Kawata, S.; Hiramata, M. *Chem. Lett.* **1998**, 959. (i) Alabugin, I. V.; Manoharan, M. *J. Phys. Chem. A* **2003**, *107*, 3363. (j) Alabugin, I. V.; Breiner, B.; Manoharan, M. *Adv. Phys. Org. Chem.* **2007**, *42*, 1. For the analysis of electronic consequences of strain, see: (k) Tykwinski, R. R. *Chem. Commun.* **1999**, 905. For the contrasting effects of strain in alkyne cyclizations, see: (l) Alabugin, I. V.; Manoharan, M. *J. Am. Chem. Soc.* **2005**, *127*, 12583. (m) Alabugin, I. V.; Manoharan, M. *J. Am. Chem. Soc.* **2005**, *127*, 9534. (n) Gilmore, K.; Alabugin, I. V. *Chem. Rev.* **2011**, *111*, 6513. (o) Vasilevsky, S. F.; Gold, B.; Mikhailovskaya, T. F.; Alabugin, I. V. *J. Phys. Org. Chem.* **2012**, *25*, 998.
- (24) Zhang, X.; Houk, K. N. *Acc. Chem. Res.* **2005**, *38*, 379.
- (25) Baskin, J. M.; Prescher, J. A.; Laughlin, S. T.; Agard, N. J.; Chang, P. V.; Miller, I. A.; Lo, A.; Codelli, J. A.; Bertozzi, C. R. *Proc. Natl. Acad. Sci. U.S.A.* **2007**, *104*, 16793.
- (26) (a) Ess, D. H.; Jones, G. O.; Houk, K. N. *Org. Lett.* **2008**, *10*, 1633. (b) Schoenebeck, F.; Ess, D. H.; Jones, G. O.; Houk, K. N. *J. Am. Chem. Soc.* **2009**, *131*, 8121. See also: (c) Chenoweth, K.; Chenoweth, D.; Goddard, W. A., III. *Org. Biomol. Chem.* **2009**, *7*, 5255. (d) Bach, R. D. J. *J. Am. Chem. Soc.* **2009**, *131*, 5233.
- (27) Gold, B.; Schevchenko, N.; Bonus, N.; Dudley, G. B.; Alabugin, I. V. *J. Org. Chem.* **2012**, *77*, 75.
- (28) This effect is similar to the electronic origin of torquoselectivity in electrocyclic reactions, where similar interactions provide selective stabilization to the TS because of the increased donor and acceptor ability of chemical bonds upon their distortion and breaking. (a) Dolbier, W. R., Jr.; Koroniak, H.; Houk, K. N.; Sheu, C. *Acc. Chem. Res.* **1996**, *29*, 471. (b) Kirmse, W.; Rondan, N. G.; Houk, K. N. *J. Am. Chem. Soc.* **1984**, *106*, 7989.
- (29) Frisch, M. J.; Trucks, G. W.; Schlegel, H. B.; Scuseria, G. E.; Robb, M. A.; Cheeseman, J. R.; Montgomery, J. A., Jr.; Vreven, T.; Kudin, K. N.; Burant, J. C.; Millam, J. M.; Iyengar, S. S.; Tomasi, J.; Barone, V.; Mennucci, B.; Cossi, M.; Scalmani, G.; Rega, N.; Petersson, G. A.; Nakatsuji, H.; Hada, M.; Ehara, M.; Toyota, K.; Fukuda, R.; Hasegawa, J.; Ishida, M.; Nakajima, T.; Honda, Y.; Kitao, O.; Nakai, H.; Klene, M.; Li, X.; Knox, J. E.; Hratchian, H. P.; Cross, J. B.; Adamo, C.; Jaramillo, J.; Gomperts, R.; Stratmann, R. E.; Yazyev, O.; Austin, A. J.; Cammi, R.; Pomelli, C.; Ochterski, J. W.; Ayala, P. Y.; Morokuma, K.; Voth, G. A.; Salvador, P.; Dannenberg, J. J.; Zakrzewski, V. G.; Dapprich, S.; Daniels, A. D.; Strain, M. C.; Farkas, O.; Malick, D. K.; Rabuck, A. D.; Raghavachari, K.; Foresman, J. B.; Ortiz, J. V.; Cui, Q.; Baboul, A. G.; Clifford, S.; Cioslowski, J.; Stefanov, B. B.; Liu, G.; Liashenko, A.; Piskorz, P.; Komaromi, I.; Martin, R. L.; Fox, D. J.; Keith, T.; Al-Laham, M. A.; Peng, C. Y.; Nanayakkara, A.; Challacombe, M.; Gill, P. M. W.; Johnson, B.; Chen, W.; Wong, M. W.; Gonzalez, C.; Pople, J. A. *Gaussian 03*, Revision C.02; Gaussian: Wallingford, CT, 2004.
- (30) Ess, D. H.; Houk, K. N. *J. Phys. Chem. A* **2005**, *109*, 9542.
- (31) (a) Miertuš, S.; Scrocco, E.; Tomasi, J. *Chem. Phys.* **1981**, *55*, 117. (b) Cossi, M.; Rega, N.; Scalmani, G.; Barone, V. *J. Comput. Chem.* **2003**, *24*, 669.
- (32) NBO 4.0. Glendening, E. D.; Badenhoop, J. K.; Reed, A. E.; Carpenter, J. E.; Weinhold, F. *Theoretical Chemistry Institute*; University of Wisconsin: Madison, WI, 1996.
- (33) For selected examples, see: (a) Vasilevsky, S. F.; Mikhailovskaya, T. F.; Mamatyuk, V. I.; Bogdanchikov, G. A.; Manoharan, M.; Alabugin, I. V. *J. Org. Chem.* **2009**, *74*, 8106. (b) Alabugin, I. V.; Manoharan, M. *J. Org. Chem.* **2004**, *69*, 9011. (c) Alabugin, I. V.; Manoharan, M.; Zeidan, T. A. *J. Am. Chem. Soc.* **2003**, *125*, 14014. (d) Alabugin, I. V.; Manoharan, M.; Peabody, S.; Weinhold, F. *J. Am. Chem. Soc.* **2003**, *125*, 5973.
- (34) Reed, A. E.; Curtiss, L. A.; Weinhold, F. *Chem. Rev.* **1988**, *88*, 899.
- (35) Previously we have shown that the hyperconjugative energies estimated by second order perturbation and deletion approaches agree

well with each other. Alabugin, I. V.; Zeidan, T. A. *J. Am. Chem. Soc.* **2002**, *124*, 3175.

(36) (a) Weinhold, F. *Encyclopedia of Computational Chemistry*; Schleyer, P. v. R., Ed.; John Wiley & Sons: New-York, 1998; Vol. 3, p 1972. (b) See also: www.chem.wisc.edu/~nbo5.

(37) Reed, A. E.; Weinhold, F. *J. Chem. Phys.* **1985**, *83*, 1736.

(38) (a) Curtin, D. Y. *Rec. Chem. Prog* **1954**, *15*, 111. (b) Hammett, L. P. *Physical Organic Chemistry*; McGraw-Hill: New York, 1970; Chapter 5. (c) Seeman, J. I. *Chem. Rev.* **1983**, *83*, 83.

(39) Taylor, M. T.; Blackman, M. L.; Dmitrenko, O.; Fox, J. M. *J. Am. Chem. Soc.* **2011**, *133*, 9646.

(40) All strain energies (SEs) are corrected for the nonzero SE of cyclohexane (2.2 kcal/mol) as suggested by Bach in ref 26d.

(41) Because carbon used more p-character in bonds to electronegative elements (the C–F bonds are $sp^{4.13}$ and $sp^{4.22}$), the C–C bonds have more s-character ($sp^{2.15}$ and $sp^{2.37}$ in DIFO). For a recent discussion of rehybridization effects in organic chemistry, see: (a) Alabugin, I. V.; Manoharan, M. *J. Comput. Chem.* **2007**, *28*, 373. For an interesting recent example, see: (b) Song, M. G.; Sheridan, R. S. *J. Phys. Org. Chem.* **2011**, *24*, 889.

(42) The only deviation from this general trend is shown in the bis-protonated endocyclic amines which show much larger (43–45 kcal/mol) SE values in the gas-phase calculations. This effect is clearly due to the Coulombic repulsion, and, not surprisingly, the SE dramatically decreases once solvation is introduced in the computational model. For an analysis of electrostatic effects imposed by ammonium substitution, see: Bach, R. D.; Dmitrenko, O.; Glukhovtsev, M. N. *J. Am. Chem. Soc.* **2001**, *123*, 7134.

(43) See also: Engler, E. M.; Androse, J. D.; Schleyer, P.; von, R. *J. Am. Chem. Soc.* **1973**, *95*, 8005.

(44) Thiacycloalkynes have recently been reported, but optimal overlap with the in plane π -system was not possible, as the heteroatoms were not in the propargylic position. The aim was to alleviate strain, and thus increase stability in cyclooctynes by incorporating a longer C–S bond in the ring. The subsequent loss of reactivity prompted investigation of thiacycloheptynes: de Almeida, G.; Sletten, E. M.; Nakamura, H.; Palaniappan, K. K.; Bertozzi, C. R. *Angew. Chem., Int. Ed.* **2012**, *51*, 2443.

(45) Alabugin, I. V.; Gilmore, K.; Peterson, P. *WIREs Comput. Mol. Sci.* **2011**, *1*, 109.

(46) Bertozzi and co-workers utilized polarity and water solubility of azacyclooct-4-yne to reduce nonspecific binding, and improve the sensitivity of azide detection in vivo: (a) Sletten, E. M.; Bertozzi, C. R. *Org. Lett.* **2008**, *10*, 3097. For another biochemical application of chemical reactions controlled via selective amine protonation, see: (b) Yang, W.-Y.; Roy, S.; A., R.; Phrathep, B.; Rengert, Z.; Alabugin, I. V. *J. Med. Chem.* **2011**, *54*, 8501. (c) Yang, W.-Y.; Marrone, S. A.; Minors, N.; Zorio, D. A. R.; Alabugin, I. V. *Beilstein J. Org. Chem.* **2011**, *7*, 813. (d) Yang, W.-Y.; Breiner, B.; Kovalenko, S. V.; Ben, C.; Singh, M.; LeGrand, S. N.; Sang, A. Q.-X.; Strouse, G. F.; Copland, J. A.; Alabugin, I. V. *J. Am. Chem. Soc.* **2009**, *131*, 11458. (e) Breiner, B.; Schlatterer, J. C.; Kovalenko, S. V.; Greenbaum, N. L.; Alabugin, I. V. *Angew. Chem., Int. Ed.* **2006**, *45*, 3666. (f) Breiner, B.; Kaya, K.; Roy, S.; Yang, W.-Y.; Alabugin, I. V. *Org. Biomol. Chem.* **2012**, *10*, 3974.

(47) (a) Alabugin, I. V.; Manoharan, M. *J. Phys. Chem. A* **2003**, *107*, 3363. (b) Alabugin, I. V.; Manoharan, M.; Kovalenko, S. V. *Org. Lett.* **2002**, *4*, 1119.

(48) (a) Ess, D. H.; Houk, K. N. *J. Am. Chem. Soc.* **2007**, *129*, 10646. (b) Hayden, A. E.; Houk, K. N. *J. Am. Chem. Soc.* **2009**, *131*, 4084. (c) Jones, G. O.; Houk, K. N. *J. Org. Chem.* **2008**, *73*, 1333. (d) Ess, D. H.; Houk, K. N. *J. Am. Chem. Soc.* **2008**, *130*, 10187. (e) Xu, L.; Doubleday, C. E.; Houk, K. N. *Angew. Chem., Int. Ed.* **2009**, *48*, 2746. (f) Lan, Y.; Houk, K. N. *J. Am. Chem. Soc.* **2010**, *132*, 17921. (g) Krenske, E. H.; Houk, K. N.; Holmes, A. B.; Thompson, J. *Tetrahedron Lett.* **2011**, *52*, 2181. (h) Krenske, E. H.; Pryor, W. A.; Houk, K. N. *J. Org. Chem.* **2009**, *74*, 5356. (i) Osuna, S.; Houk, K. N. *Chem.—Eur. J.* **2009**, *15*, 13219. (j) additions to graphene: Cau, Y.; Houk, K. N. *J. Mater. Chem.* **2011**, *21*, 1503. (k) addition of metals: Ess, D. H. *J. Org. Chem.* **2009**, *74*, 1498. (l) expansion to

intermolecular reactions: Krenske, E. H.; Davison, E. C.; Forbes, I. T.; Warner, J. A.; Smith, A. L.; Holmes, A. B.; Houk, K. N. *J. Am. Chem. Soc.* **2012**, *134*, 2434. For related activation strain concept, see: (m) Bickelhaupt, F. M.; Ziegler, T.; Schleyer, P. v. R. *Organometallics* **1995**, *14*, 2288. (n) Bickelhaupt, F. M. *J. Comput. Chem.* **1999**, *20*, 114. (o) Diefenbach, A.; Bickelhaupt, F. M. *J. Chem. Phys.* **2001**, *115*, 4030. (p) Diefenbach, A.; Bickelhaupt, F. M. *J. Phys. Chem. A* **2004**, *108*, 8460. (q) de Jong, G. T.; Bickelhaupt, F. M. *Chem. Phys. Chem.* **2007**, *8*, 1170.

(49) As a consequence, the other C–F bond is moved to the position where it overlaps better with the π_{out} orbital.

(50) Another structural effect associated with the CF_2 group is the unusually large 109.6 °CCC angle at the fluorinated propargylic carbon (compare with 107.0 ° in OCT). This effect is another consequence of rehybridization associated with the Bent's rule.

(51) Alabugin, I. V.; Manoharan, M. *J. Am. Chem. Soc.* **2003**, *125*, 4495.

(52) This is possible because the dominant Lewis structure in the TS corresponds to the separated azide and alkyne moieties.

(53) This indicates that endocyclic acceptors also stabilize the reactant which may facilitate preparation and overall stability of such bent alkynes.

(54) Note that the effect of two propargylic C–F bonds in the 1,5-TS includes not only the C–H \cdots F interactions but also a contribution from 1,5-hyperconjugative assistance. Separation of these effects is not among the aims of the present manuscript.

(55) An example is given in the Supporting Information. The full analysis of these complexes extends beyond the scope of the present manuscript.